16th World Congress in Computational Mechanics (WCCM)
21-26 July 2024, Vancouver, Canada
A. Korobenko, M. Laforest, S. Prudhomme, R. Vaziri (Eds)

COMPUTATIONAL MODEL FOR LOCAL BUCKLING OF COMPRESSIVELY LOADED OMEGA-STRINGER-STIFFENED PANELS

C. EL YAAKOUBI-MESBAH[1], C. MITTELSTEDT[2]

[1] TU Darmstadt, Faculty of Mechanical Engineering
Otto-Berndt-Str. 2, 64287 Darmstadt, Germany
cherine.mesbah@lsm.tu-darmstadt.de

[2] TU Darmstadt, Faculty of Mechanical Engineering
Otto-Berndt-Str. 2, 64287 Darmstadt, Germany
christian.mittelstedt@lsm.tu-darmstadt.de

Key words: Composites, Omega-stringer, Local buckling, Closed-form analysis

Abstract. Thin-walled composite structures are used in applications such as aircraft and spacecraft due to their low weight and corresponding high stiffness properties. To optimize the potential of these structures to the fullest extent, a complete understanding of their stability behavior is required. Thereby, uniaxial compression describes an important load case that is investigated. A closed-form analytical method based on the energy method for determining the local buckling load of omega-stringer-stiffened panels is presented. The stiffened panel under consideration consists of the skin plate with eccentrically attached stringer feet along the longitudinal sides of the panel, while the remaining part of the omega-stringer is modeled by corresponding elastically restrained edges. Due to the applied stringer feet, stiffness discontinuities occur in the stiffened panel. This is covered by the presented method, whereas in comparable studies in the literature, a homogeneous stiffness is often assumed across the entire panel. To evaluate the new analysis method, a comparison with the numerical solution of the corresponding Lévy-type solution and the finite element analysis is being drawn.

1 INTRODUCTION

Stiffened composite panels are employed in a multitude of applications, such as aircraft fuselages [1]. The subject of this study are panels stiffened with omega stringers, for which an analysis of their stability behavior is necessary, as they possess a high degree of flexibility due to their thin-walled structure. Given that numerous configurations are often investigated in parameter studies during the early stages of development, a closed-form analytical computational model is required. The current contribution presents a closed-form analytical approach for the determination of local buckling loads of omega-stringer-stiffened panels. Figure 1 illustrates a unit cell of such a panel.

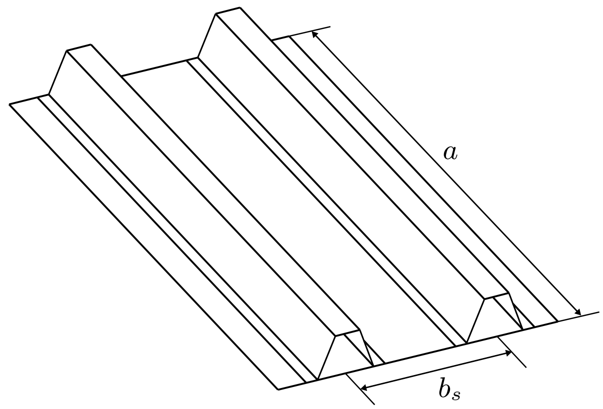

Figure 1: Exemplary unit cell of an omega-stringer-stiffened panel.

There are three principal approaches to modeling the coupling between the stringer and the adjacent skin plate. In the most basic approach, the influence of the stringer is neglected and the corresponding edge is assumed as simply supported. The second approach was employed by Vescovini and Bisagni [2] and entails the complete modeling of the stringer, which is defined by a corresponding shape function for each subplate. In the final approach, the stringer is replaced by rotational elastic restraints along the edges [3, 4]. This approach allows for a more rapid calculation of the local buckling load, as the modeling of the stringer is no longer necessary. The spring stiffnesses are determined using the principle of virtual work and depend only on the geometric and material properties of the stringer.

Another issue that must be addressed in the context of omega-stringer-stiffened panels is the modeling of the stringer feet. The eccentrically attached stringer foot causes discontinuities in the stiffnesses and thus discontinuities in the curvature behavior of the structure. Therefore, this effect should be taken into account. There are various approaches in the literature for considering the different stiffnesses. Herencia et al. [5] consider the different stiffnesses when calculating the elastic potential, but only define one global approach function for the panel. Schilling and Mittelstedt [6] provide the most recent approach by segmenting the model into different subplates and defining the corresponding approach functions, which are coupled with each other via continuity conditions.

2 CLOSED-FORM ANALYTICAL APPROACH

2.1 Introduction

In this work, a closed-form analytical approach for determining the critical buckling load of panels braced by omega-stringer based on the energy method is presented. To avoid having to define shape functions for every plate segment of the panel, a reduced model is used, as shown in Figure 2. The unit cell contains the stringer foot attached to the skin plate, while the stringer itself is modeled using rotational elastic restraints along the longitudinal edge. The unit cell is subjected to uniaxial compression N_{xx}^0. To reduce the effort, symmetry properties of the panel are considered.

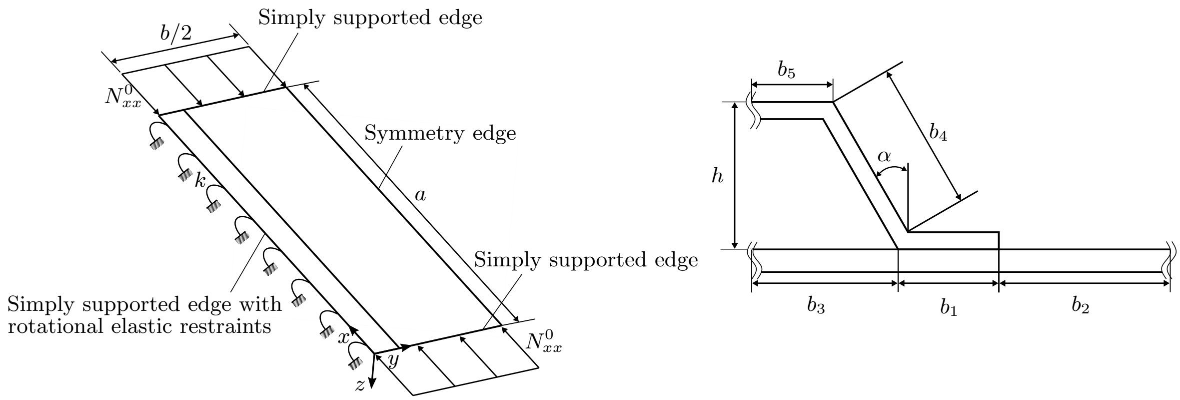

Figure 2: Reduced model with elastic restraints along the edge subjected to uniaxial compression (left) and side-view on the model with geometrical quantities (right).

The classical laminated plate theory (CLPT), which is appropriate for thin laminates and neglects transverse shear deformation, is used to describe the behavior of the laminates in the following. A detailed overview of this theory can be found in textbooks like [7, 8, 9]. Furthermore, only symmetric and orthotropic laminates are investigated.

The restraint stiffnesses of the rotational elastic restraints along the longitudinal edges are determined from geometry and material properties of the stringer using the virtual work method. Therefore, the stringer is treated as a plate assembly consisting of three subplates. A detailed description of the methodology can be found in the work of Mittelstedt and Beerhorst [4].

2.2 Partitioning

The determination of the local buckling load of a panel stiffened with omega-stringers is based on an unit cell, in which only the stringer foot attached to the skin plate and the skin plate are considered, while the stringer is modeled as rotational elastic restraints along the edges. Figure 3 shows the partitioning of the reduced model, where two subplates are considered: the assembly of skin plate and stringer foot (1) and the skin plate (2) itself.

Due to the eccentrically attached stringer foot, the stiffnesses of subplate (1) must first be determined as presented in Eq. (1). These result from those of the skin plate (2) and the stringer foot laminate (f).

$$\begin{bmatrix} \underline{\underline{A}} & \underline{\underline{B}} \\ \underline{\underline{B}} & \underline{\underline{D}} \end{bmatrix}_1 = \begin{bmatrix} \underline{\underline{A}} & \underline{\underline{B}} \\ \underline{\underline{B}} & \underline{\underline{D}} \end{bmatrix}_2 + \begin{bmatrix} \underline{\underline{A}}_f & \underline{\underline{B}}_f + e\underline{\underline{A}}_f \\ \underline{\underline{B}}_f + e\underline{\underline{A}}_f & \underline{\underline{D}}_f + 2e\underline{\underline{B}}_f + e^2\underline{\underline{A}}_f \end{bmatrix} \tag{1}$$

Although all individual laminates are symmetrical, the bonding results in an asymmetrical laminate, as the bending-extensional coupling $\underline{\underline{B}}$ does not vanish. The plate assembly (1) is approximated as symmetric using the reduced bending stiffness method (RBS). Therefore, the

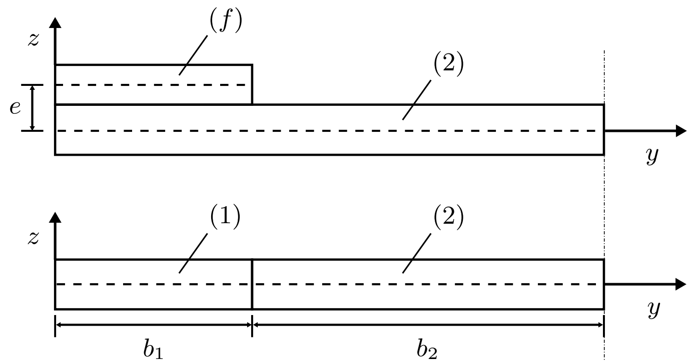

Figure 3: Partitioning of the reduced model resulting in two subplates (1) and (2) with corresponding stiffnesses.

plate stiffnesses $\underline{\underline{D}}_1$ are replaced by reduced plate stiffnesses $\underline{\underline{D}}_1^*$ according to Eq. (2), while the bending-extensional coupling $\underline{\underline{B}}_1$ is neglected [10].

$$\underline{\underline{D}}_1^* = \underline{\underline{D}}_1 - \underline{\underline{B}}_1 \, \underline{\underline{A}}_1^{-1} \underline{\underline{B}}_1 \tag{2}$$

2.3 Boundary and symmetry conditions

For the analytical model, the geometrical and dynamic boundary conditions as well as the continuity conditions are required. The superscript $()^0$ denotes that the quantities are referred to the mid-plane of the laminate. The transverse edges are loaded and simply supported, resulting in the following boundary conditions:

$$w_{0,j}(x = 0, a, y) = 0 \qquad \text{for } j = 1, 2, \tag{3}$$

$$M^0_{xx,j}(x = 0, a, y) = 0 \qquad \text{for } j = 1, 2. \tag{4}$$

The unloaded edge is simply supported with rotational restraints with the spring constant k:

$$w_{01}(x, y = 0) = 0 \tag{5}$$

$$M^0_{yy,1}(x, y = 0) = -k \frac{\partial w_{01}}{\partial y}(x, y = 0) \tag{6}$$

The transition between the two subplates is described in terms of continuity conditions, as expressed in Eqs. (7)-(10). Thus, there must be an equal deflection and rotation in addition to an equal bending moment and Kirchhoff shear force.

$$w_{01}(x, y = b_1) = w_{02}(x, y = b_1) \tag{7}$$

$$\frac{\partial w_{01}}{\partial y}(x, y = b_1) = \frac{\partial w_{02}}{\partial y}(x, y = b_1) \tag{8}$$

$$M^0_{yy,1}(x, y = b_1) = M^0_{yy,2}(x, y = b_1) \tag{9}$$

$$\bar{Q}_{y,1}(x, y = b_1) = \bar{Q}_{y,2}(x, y = b_1) \tag{10}$$

As symmetry properties were incorporated into the reduced model, it is necessary to define symmetry conditions:

$$\frac{\partial w_{02}}{\partial y}(x, y = b_1 + b_2) = 0, \tag{11}$$

$$Q_{y,2}(x, y = b_1 + b_2) = 0. \tag{12}$$

2.4 Principle of the minimum of the total elastic potential

For the defined subplates of the model, the shape functions for the deflections are defined. Polynomial, trigonometric, or a combination of these functions is often employed in buckling analyses. In the following, the approach functions expressed in Eqs. (13) and (14) will be utilized. The sine term in the x-direction with the half-wave number m fulfills the boundary conditions in Eqs. (3) and (4) identically. The two constants, A and B, are free values. The remaining constants C_{jn} $(j = 1, 2,\ n = 1, 2, 3, 4)$ are determined using the linear system of equations resulting from the boundary and continuity conditions.

$$w_{01}(x, y) = \sin\left(\frac{\pi m x}{a}\right)\left[A\left(\frac{y}{b_1}\right)^4 + C_{11}\left(\frac{y}{b_1}\right)^3 + C_{12}\left(\frac{y}{b_1}\right)^2 + C_{13}\left(\frac{y}{b_1}\right) + C_{14}\right] \tag{13}$$

$$w_{02}(x, y) = \sin\left(\frac{\pi m x}{a}\right)\left[B\left(\frac{y}{b_2}\right)^4 + C_{21}\left(\frac{y}{b_2}\right)^3 + C_{22}\left(\frac{y}{b_2}\right)^2 + C_{23}\left(\frac{y}{b_2}\right) + C_{24}\right] \tag{14}$$

The analytical computation model for determining the critical buckling load is based on the principle of the minimum of the total elastic potential. The total potential is derived from the internal potentials $\Pi_{i,j}$ and the potentials of the external loads $\Pi_{e,j}$ of both subplates j, and the potential stored in the edge springs Π_s:

$$\Pi = \sum_{j=1}^{2} (\Pi_{i,j} + \Pi_{e,j}) + \Pi_s. \tag{15}$$

Following the approach of Schilling and Mittelstedt [6], the coefficients are rewritten in respect to the free values:

$$C_{jn} = A C_{A,jn} + B C_{B,jn}, \tag{16}$$

which leads to the following expression for the buckling shape functions:

$$w_{0,j} = A w_{A,j}(x, y) + B w_{B,j}(x, y). \tag{17}$$

For symmetrical, orthotropic laminates subjected to uniaxial compression N_{cr}, the following formulations for the potentials are obtained:

$$\Pi_{i,j} = A^2\Lambda_{A,j} + AB\Lambda_{AB,j} + B^2\Lambda_{B,j} \qquad \text{for } j = 1, 2, \tag{18}$$

$$\Pi_{e,j} = A^2N_{cr}U_{A,j} + ABN_{cr}U_{AB,j} + B^2N_{cr}U_{B,j} \qquad \text{for } j = 1, 2, \tag{19}$$

$$\Pi_s = A^2Z_{A,j} + ABZ_{AB,j} + B^2Z_{B,j} \qquad \text{for } j = 1, \tag{20}$$

where

$$\begin{aligned}\Lambda_{n,j} = \frac{1}{2}\int_0^a \int_{\omega_j}^{\Omega_j} \Bigg[& D_{11,j}\left(\frac{\partial^2 w_{n,j}}{\partial x^2}\right)^2 + D_{22,j}\left(\frac{\partial^2 w_{n,j}}{\partial y^2}\right)^2 + 2D_{12,j}\frac{\partial^2 w_{n,j}}{\partial x^2}\frac{\partial^2 w_{n,j}}{\partial y^2} \\ & +4D_{66,j}\left(\frac{\partial^2 w_{n,j}}{\partial x \partial y}\right)^2\Bigg] \mathrm{d}y\mathrm{d}x \qquad \text{for } n = A, B,\end{aligned} \tag{21}$$

$$\begin{aligned}\Lambda_{AB,j} = \int_0^a \int_{\omega_j}^{\Omega_j} \Bigg[& D_{11,j}\frac{\partial^2 w_{A,j}}{\partial x^2}\frac{\partial^2 w_{B,j}}{\partial x^2} + D_{22,j}\frac{\partial^2 w_{A,j}}{\partial y^2}\frac{\partial^2 w_{B,j}}{\partial y^2} + D_{12,j}\frac{\partial^2 w_{A,j}}{\partial x^2}\frac{\partial^2 w_{B,j}}{\partial y^2} \\ & +D_{12,j}\frac{\partial^2 w_{B,j}}{\partial x^2}\frac{\partial^2 w_{A,j}}{\partial y^2} + 4D_{66,j}\frac{\partial^2 w_{A,j}}{\partial x \partial y}\frac{\partial^2 w_{B,j}}{\partial x \partial y}\Bigg] \mathrm{d}y\mathrm{d}x,\end{aligned} \tag{22}$$

$$U_{n,j} = -\frac{1}{2}\delta_j \int_0^a \int_{\omega_j}^{\Omega_j} \left(\frac{\partial w_{n,j}}{\partial x}\right)^2 \mathrm{d}y\mathrm{d}x \qquad \text{for } n = A, B, \tag{23}$$

$$U_{AB,j} = -\delta_j \int_0^a \int_{\omega_j}^{\Omega_j} \frac{\partial w_{A,j}}{\partial x}\frac{\partial w_{B,j}}{\partial x} \mathrm{d}y\mathrm{d}x, \tag{24}$$

$$Z_{n,j} = \frac{1}{2}k \int_0^a \left(\frac{\partial w_{n,j}}{\partial x}\Big|_{y=0}\right)^2 \mathrm{d}x \qquad \text{for } n = A, B, \tag{25}$$

$$Z_{AB,j} = k \int_0^a \frac{\partial w_{A,j}}{\partial x}\Big|_{y=0}\frac{\partial w_{B,j}}{\partial x}\Big|_{y=0} \mathrm{d}x. \tag{26}$$

The quantities δ_j are the load factors and describe the relationship of the loads of each plate segment $N_{xx,j}$ and the external line load N_{xx}^0, as expressed in Eq. (27). The fundamental presumption is that both plate segments have equal longitudinal elongation [11]. With this method, linear buckling for a single critical buckling load can be studied.

$$N_{xx,j} = \delta_j N_{xx}^0 \tag{27}$$

The substitute variables Γ_m, X_m and Z_m for $m = 1, 2, 3$ are computed according to Eqs. (28)-(30).

$$\Gamma_1 = \sum_{j=1}^{2} \Lambda_{A,j} \qquad \Gamma_2 = \sum_{j=1}^{2} \Lambda_{AB,j} \qquad \Gamma_3 = \sum_{j=1}^{2} \Lambda_{B,j} \tag{28}$$

$$X_1 = \sum_{j=1}^{2} U_{A,j} \qquad X_2 = \sum_{j=1}^{2} U_{AB,j} \qquad X_3 = \sum_{j=1}^{2} U_{B,j} \tag{29}$$

$$Z_1 = Z_{A,1} \qquad Z_2 = Z_{AB,1} \qquad Z_3 = Z_{B,1} \tag{30}$$

The principle of the minimum of the total elastic potential states that the first variation of the total potential has to vanish:

$$\delta\Pi = \frac{\partial\Pi}{\partial A}\delta A + \frac{\partial\Pi}{\partial B}\delta B = 0. \tag{31}$$

The first variation (Eq. 31) yields two independent Ritz-equations that constitute a linear system of equations with respect to the free values. For a nontrivial solution, the determinant of the system of equations must vanish, describing the buckling condition. The eigenvalue problem can be solved analytically, which leads to the following expression for the critical buckling load:

$$N_{cr} = -\frac{\alpha_2 \pm \sqrt{\alpha_2^2 - 4\alpha_1\alpha_3}}{2\alpha_1} \tag{32}$$

where

$$\alpha_1 = 4X_1X_3 - X_2^2$$
$$\alpha_2 = 4X_1\left(\Gamma_3 + Z_3\right) - 2X_2\left(\Gamma_2 + Z_2\right) + 4X_3\left(\Gamma_1 + Z_1\right)$$
$$\alpha_3 = 4\Gamma_1\Gamma_3 + 4\Gamma_1 Z_3 + 4Z_1\Gamma_3 + 4Z_1Z_3 - \Gamma_2^2 - Z_2^2 - 2\Gamma_2 X_2$$

The critical buckling load of the assembly is defined as the smaller value obtained from Eq. (32). The buckling load is depending on geometric and material parameters, in addition to the restraint stiffness k and the half-wave number m. In order to determine the critical buckling load, it is necessary to evaluate Eq. (32) for different half-wave numbers, with the smallest of these corresponding to the solution sought.

3 RESULTS

The closed-form analysis presented in this paper represents an approximate solution to the underlying buckling problem. In order to assess the quality of the computational model, the analytical results are compared with the exact Lévy-type solution and the numerical results of a finite element model. For the numerical model, a unit cell of a panel stiffened with omega stringer was modeled (see Figure 1) using the software Abaqus.

Figure 4 shows the results of a parameter study on the variation of the panel length a for different stringer spacings b_s. The individual curves show the typical course of buckling curves

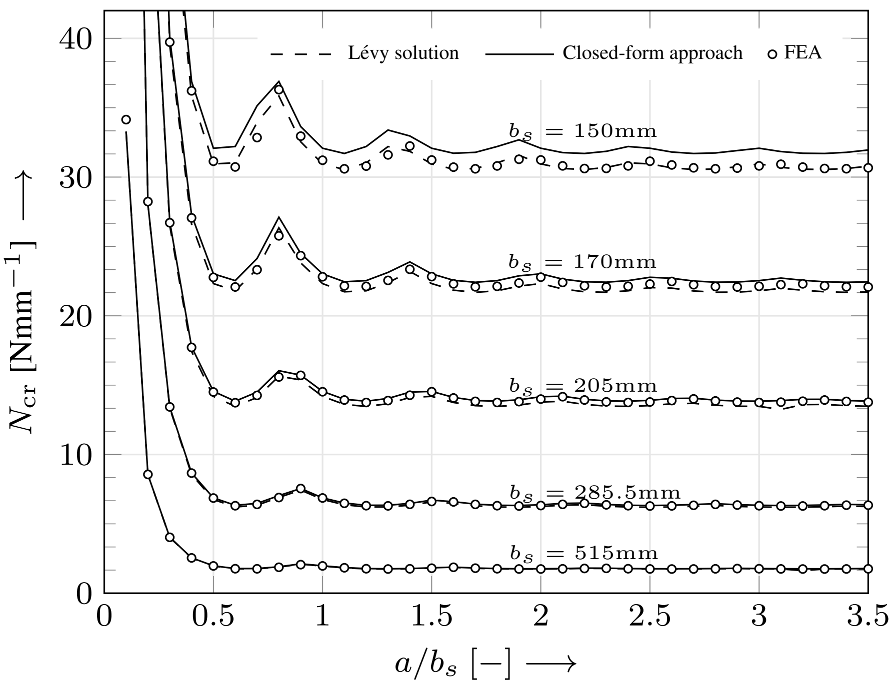

Figure 4: Buckling loads obtained by the present closed-form analysis, finite element analysis (FEA) and Lévy-type solution for different stringer spacings b_s; stringer configuration: $h = 30$mm, $\alpha = 25°, b_1 = 0.1b, b_5 = 55.5$mm; stringer layup: $[0, 90, 0, 90, 0, 90, 0]$, skin layup: $[0, 90, 0, 90]_s$; material properties: $E_1 = 150$GPa, $E_2 = 9$GPa, $G_{12} = 5.3$GPa, $\nu_{12} = 0.33$.

with local maxima describing the mode changes. The error of the numerical results and the Lévy solution ranges from about -3.8% to about 1.7%. For larger spacings ($b_s \geq 205$mm), a very satisfactory agreement of the results can be seen. The maximum error of the closed-form analysis observed in this instance is $\varepsilon = 2.9\%$. For smaller distances, a deviation can be observed in the results, with an average error of $\varepsilon = 3.4\%$ for $b_s = 150$mm. The discrepancy can be attributed to the calculation of the spring stiffness, which is solely dependent on the geometry and material parameters of the stringer. The buckling of the skin under the stringer, which occurs more frequently at smaller distances b_s, is not included in the calculation. The deviation can be reduced in these cases by neglecting the skin under the stringer when calculating the restraint stiffness.

The results of the variation of the stringer web angle α are presented in Figure 5 for different stringer spacings b_s. In all cases, the analytical approximate solution overestimates the critical buckling load by the finite element analyses (FEA). It is noteworthy that the load to be withstood is almost independent of the angle. As in the previous parameter study, the results here demonstrate excellent agreement for $b_s \geq 170$mm with an average deviation of $\varepsilon = 0.75\%$. A maximum deviation of $\varepsilon = 4.45\%$ can be observed for $b_s = 150$mm.

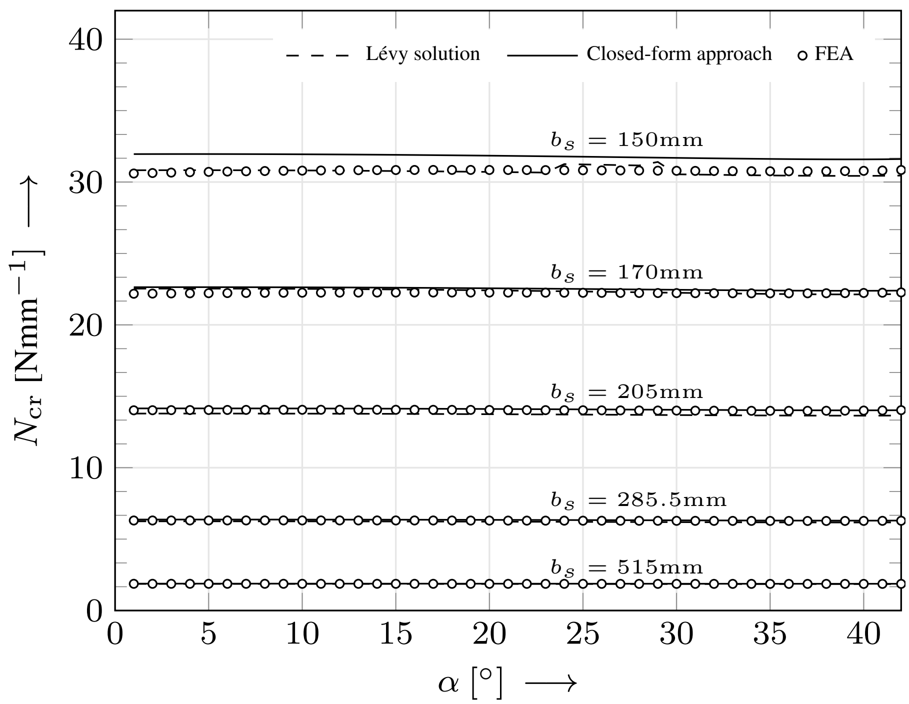

Figure 5: Comparison on the buckling load for a variation of the stringer web angle α for different stringer spacings b_s; stringer configuration: $h = 30\text{mm}, \alpha = 25°, b_1 = 0.1b, b_5 = 55.5\text{mm}$; stringer layup: $[0, 90, 0, 90, 0, 90, 0]$, skin layup: $[0, 90, 0, 90]_s$; material properties: $E_1 = 150\text{GPa}, E_2 = 9\text{GPa}, G_{12} = 5.3\text{GPa}, \nu_{12} = 0.33$.

4 CONCLUSIONS

In this work, a closed-form analysis was presented to describe the local buckling behavior of stiffened panels using a reduced model. The discontinuities in the stiffnesses caused by the eccentrically attached stringer feet are taken into account. The stringer is modeled as rotational elastic restraints, where the restraint stiffnesses are calculated using the principle of virtual work. Using a Ritz-like approach and the principle of the minimum of the total elastic potential, the critical buckling load is expressed in an explicit form. The analytical results show very good agreement with the Lévy solution and the numerical results, particularly when the skin plate is the most critical plate in the assembly. Due to the concept of modeling the stringer as springs, the work presented is not limited to omega-stringers and can be extended to other stringer configurations. The model allows for the effective and rapid calculation of the critical buckling load, which is particularly advantageous in parameter studies during the design phase.

REFERENCES

[1] ATK. ATK delivers A350 parts. *Reinforced Plastics* (2010) **54**:12.

[2] Vescovini, R. and Bisagni, C. Semi-analytical buckling analysis of omega stiffened panels under multi-axial loads. *Composite Structures* (2015) **120**:285–299.

[3] Mittelstedt, C. Closed-form buckling analysis of stiffened composite plates and identification of minimum stiffener requirements. *International Journal of Engineering Science* (2008) **46**:1011–1034.

[4] Mittelstedt, C. and Beerhorst, M. Closed-form buckling analysis of compressively loaded composite plates braced by omega-stringers. *Composite Structures* (2009) **88**:424–435.

[5] Herencia, J. and Weaver, P. and Friswell, M. Optimisation of anisotropic plates that vary in thicknesses and properties. *ICCM International Conferences on Composite Materials* (2007).

[6] Schilling, J. and Mittelstedt, C. Local buckling analysis of omega-stringer-stiffened composite panels using a new closed-form analytical approximate solution. *Thin-Walled Structures* (2020) **147**:106534.

[7] Jones, R. M. Mechanics of Composite Materials. *Taylor and Francis* (1999) 2nd ed.

[8] Reddy, J. N. Mechanics of laminated composite plates and shells: theory and analysis. *CRC Press* (2004) 2nd ed.

[9] Mittelstedt, C. and Becker, W. Strukturmechanik ebener Laminate. Studienbereich Mechanik, Technische Universitat Darmstadt (2016) 1st ed.

[10] Reissner, E. and Stavsky, Y. Bending and stretching of certain types of heterogeneous aeolotropic elastic plates. *Journal of Applied Mechanics* (1961) **28**:402–408.

[11] Mittelstedt, C. Explicit local buckling analysis of stiffened composite plates accounting for periodic boundary conditions and stiffener–plate interaction. *Composite Structures* (2009) **91**:249–265.